Dynamic phase transitions in confined lubricant fluids under shear

Carlos Drummond* and Jacob Israelachvili
Department of Chemical Engineering, Materials Department, and Materials Research Laboratory, University of California, Santa Barbara, California 93106

(Received 7 April 2000; published 27 March 2001)

A surface force apparatus was used to measure the transient and steady-state friction forces between molecularly smooth mica surfaces confining thin films of squalane, $C_{30}H_{62}$, a saturated, branched hydrocarbon liquid. The dynamic friction ''phase diagram'' was determined under different shearing conditions, especially the transitions between stick-slip and smooth sliding ''states'' that exhibited a chaotic stick-slip regime. The apparently very different friction traces exhibited by simple spherical, linear, and branched hydrocarbon films under shear are shown to be due to the much longer relaxation times and characteristic length scales associated with transitions from rest to steady-state sliding, and vice versa, in the case of branched liquids. The physical reasons and tribological implications for the different types of transitions observed with spherical, linear, and branched fluids are discussed.

DOI: 10.1103/PhysRevE.63.041506 PACS number(s): 62.20.Fe, 62.40.+i, 64.70.Fx, 68.15.+e

INTRODUCTION

Most oil-based lubricant fluids are branched rather than straight chain hydrocarbons. The reason for this is believed to be the inability of irregularly shaped branched molecules to freeze or solidify when confined between two surfaces since this would raise their friction to very high values [1]. However, in spite of sophisticated instruments [1–3] and computers [4] that allow the study of tribological problems with unprecedented depth and accuracy, the factors that determine whether a liquid will perform as a good lubricant are still far from being understood. One reason why friction measurements are difficult to interpret is that one cannot easily dissociate the properties of the sheared fluid film from the properties of the system, the machine or measuring apparatus through which the friction forces and their effects are detected or ''felt.'' This is because to measure the friction force between two rubbing objects, it is necessary to couple the shearing surfaces to a compliant element whose deformation will indicate the resistance to sliding. The simplest mechanical model representing the measuring process is presented in Fig. 1. The compliant element (represented here by a spring) is typically driven at constant velocity V with the laboratory acting as the inertial frame of reference. In general, the driver velocity V is not identical to the instantaneous relative sliding velocity of the rubbing surfaces V_i (where the subscript i refers to the *interfacial* or *intrinsic* value). In addition, the *measured* friction force F, as measured from the deflection of the friction spring, is not the same as the actual friction force F_i acting at that instant between the surfaces. However, by measuring the spring deflection at time t, both the position of the sliding upper surface x and the friction force F_i between the surfaces can be calculated by solving

$$m\ddot{x} = F_i(t) - K[x(t) - Vt], \tag{1}$$

where the measured and interfacial friction forces, F and F_i, are related by

$$F(t) = K[x(t) - Vt] = F_i(t) - m\ddot{x}, \tag{2}$$

where m is the mass of the sliding surface, $[Vt - x(t)]$ is the deflection of the spring from its equilibrium position, and the overdots denote time derivatives. In a typical tribological experiment (or a tribological system such as an engine), one typically measures the deflection of the friction spring (e.g., the shaft in an engine) from which the intrinsic friction force is obtained or detected. As can be inferred from Eqs. (1) and (2), the mechanical properties of the system, e.g., the spring stiffness K and inertial mass m, will influence the results. In particular, a characteristic inertial time scale $\tau_{\mathrm{mech}} = 2\pi(m/K)^{1/2}$ associated with the resonance frequency of the mass-spring system enters naturally into the equations. If the inertial term $m\ddot{x}$ in Eq. (1) can be neglected, i.e., if the sliding velocity V_i is sufficiently slow at all times, the instantaneous friction force between the surfaces $F_i(t)$ can be obtained directly from the deflection of the spring as

$$F_i(t) = F(t) = K[x(t) - Vt], \tag{3}$$

i.e., the measured force $F(t)$ is the same as the true friction force $F_i(t)$ acting between the surfaces. Equation (3) is deceptively simple, but the instantaneous friction force $F_i(t)$ can be a complicated function of several parameters, including the temperature T, normal load L, driving velocity V, and, most importantly, the previous history of the sliding surfaces [5]. In such cases, one cannot characterize the friction behavior in terms of a coefficient of friction, $\mu = F/L$, even one that is allowed to depend on the load, sliding velocity, and temperature. A detailed description of the previous sliding history is also required to obtain a complete picture of the shear process, for example to be able to determine how the system will behave under a specific change of sliding conditions.

To what extent the previous sliding history is important for describing boundary lubrication appears to depend on the nature of the lubricant used (although viscoelastic relaxations of the substrate surfaces can also play a role). Simple liquid

*Present address: PDVSA INTEVEP, P.O. Box 76343, Caracas 1070-A, Venezuela.

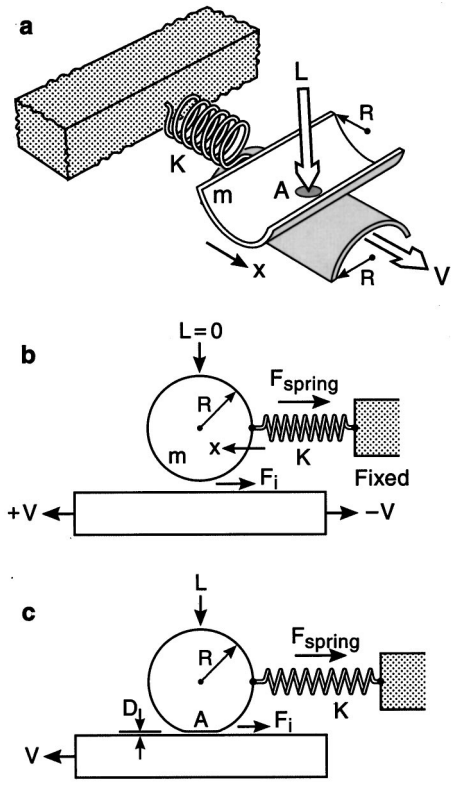

FIG. 1. Schematic geometry of the friction experiments with the surface forces apparatus (SFA). When the two mica surfaces are pressed into contact under a normal load L, the glue layers used to attach the mica sheets to the silica lenses of radii R undergo elastic deformation. A circular area of contact A confines a thin film of thickness D. The lower surface is driven laterally at velocity V. The lateral movement x induced in the upper surface, which is attached to a displacement-sensing spring of stiffness K, determines the measured friction force F, where F_i is the real or *interfacial* friction force. The equivalent sphere on plate geometry is presented below.

lubricants, consisting of small spherical or short linear chain molecules, have fast relaxation processes that allow the sheared film to evolve quickly to its steady-state sliding conditions. In such cases, the problem is greatly simplified and the classical two-parameter description, first proposed by Coulomb [6], in terms of a static force F_s at zero sliding velocity (i.e., the force needed to initiate sliding) and a smaller kinetic force F_k at finite sliding velocities (i.e., during sliding) satisfactorily accounts for observed behavior at low and moderate sliding velocities.

With more complex but more realistic fluids, this simple description no longer applies. Long memory effects have been observed [5,7] with branched hydrocarbon molecules even when the degree of branching is low (one or two side groups per molecule). For such fluids, the frictional force strongly depends on the previous shear history, and a different descriptive approach has to be taken. One of these is the use of ''friction maps'' or ''dynamic phase diagrams'' [8]. This approach considers the dependence of the ''equilibrium'' or *steady-state* friction force on different variables, but not the dynamics (transition process) of the force to its steady-state value, which can be very slow. Carlson and Batista [9] introduced the idea of using a ''rate and state'' model to describe the frictional behavior of lubricated single asperity contacts [as used in the surface force apparatus (SFA)] as was done before by Dietrich and by Ruina [10] to describe the friction of rocks. Their phenomenological approach accounts for previous time and other transient effects and has given satisfactory results for short linear chain hydrocarbons; but as we shall see here, the model needs to be expanded to explain the behavior of more complex lubricant fluids. The Thompson and Robbins molecular-dynamics simulation [11] of two shearing surfaces that confine simple spherical molecules between them revealed a very rich behavior involving a transition from stick-slip to smooth sliding with increasing sliding velocity via a chaotic regime (cf. Fig. 3 in Ref. [11]). Persson [12] has proposed the use of a thermally activated two-dimensional model of pinned islands in the contact region, analogous to the Burridge-Knopoff model [13], to describe the behavior of confined lubricants under shear, with very promising results. Klafter and coworkers [14] also proposed the use of a simple model to describe the frictional behavior of thin films of chain molecules. Their model, which displays many qualitative similarities with real films under shear, consists of rigid walls interacting via a periodic potential with a single particle or a chain of identical particles. Even though many of the above models are able to reproduce some of the physics of the problem, it is usually unclear how to relate the parameters in the models with molecular properties or with the experimentally measurable quantities.

Smooth and stick-slip steady-state sliding

When a lubricant film is subjected to shear, very rich dynamic behavior is often observed. In general, two very different steady-state sliding regimes are found depending on the conditions. In the first, the measured friction force is constant, with small fluctuations around an average value. This behavior is known as ''smooth sliding.'' In the second, at different experimental conditions, the measured force (and spring deflection) oscillates regularly between two extrema that are generally referred to as the ''static'' and ''kinetic'' friction forces when measuring at overdamped conditions. This is referred to as ''stick-slip'' sliding [15].

The transition from one dynamic sliding state to the other (stick-slip to smooth sliding or vice versa) can be driven by changes in the boundary layer (the lubricant fluid or surface layer or roughness), the mechanical setup (the spring or material stiffness K and/or the mass of the moving surfaces m), or the experimental conditions during sliding (the load L, driving velocity V, ambient temperature T, relative humidity, etc.). Systematically studying the dynamic phase diagram, for example measuring F versus V, can reveal interesting details, even at the molecular level, of confined liquid films under shear.

The self-sustained oscillating regime of stick-slip can appear for different reasons, as has been described by Yoshizawa and Israelachvili [16], Berman *et al.* [17], and Persson [18]. Some of the possible mechanisms are related to inertial effects of the whole system, where the characteristic

time of the slip is the *system's* relaxation time τ_{mech} (this is known as *underdamped* stick slip). At the opposite extreme, when the fluid film exhibits long relaxation times ($\tau_{\mathrm{film}} \gg \tau_{\mathrm{mech}}$), the stick slip is independent of the system's inertia and becomes determined by the properties of the film (known as *overdamped* conditions). In this paper, we discuss the stick-slip to smooth sliding transitions in different overdamped systems.

EXPERIMENT

The experiments described in this paper were performed with an SFA3 modified for friction studies, which has been described elsewhere [19,20]. Back-silvered molecularly smooth mica surfaces are glued to silica lenses, and are used to confine liquid films of the lubricants under study. The cylindrically shaped silica disks are placed with their axes perpendicular to each other. If the separation between the cylindrical surfaces is much smaller than their radii of curvature, R, this configuration is equivalent to a sphere on plate contact, as shown in Fig. 1. When the mica surfaces are brought into contact under a controlled normal load L, the glue layer under each sheet deforms elastically, and the thin lubricant films are confined to a uniform thickness D over a circular area A. The film thickness and the size of the contact can be measured using multiple beam interferometry [21].

A bimorph slider [20] is used to drive the lower surface at constant velocity, V. The upper surface is attached to a double cantilever spring whose deflection is monitored using semiconductor strain gauges. In this way the lateral position of the upper surface x, can be determined with an accuracy of 50 Å during the experiment.

We studied thin films of 2,6,10,15,19,23 hexamethyltetracosane (squalane) provided by Exxon Lube Technology Research division (Clinton, NJ). The lubricant was filtered with a membrane of pore size 0.25 μm before being used in order to remove undesired particles; otherwise, it was used as received. Prior to injecting a lubricant droplet between the two clean mica surfaces, the apparatus was purged with dry nitrogen gas for 8 h. After injecting 100 μl of the lubricant between the mica surfaces, a small amount of phosphorus pentoxide (P_2O_5) was placed inside the apparatus chamber to maintain dry conditions throughout the experiment. The system was allowed to thermally equilibrate (typically 2–3 h) prior to every experiment. The temperature was controlled within 0.1 °C, and the normal load L within 10 μN.

Previous experimental results

The shear behavior of thin films of squalane has been studied several times in the past. Demirel and Granick [22] conducted experiments driving the rubbing surfaces with a low amplitude sinusoidal excitation and observed long correlation times in the friction force fluctuations and a power-law scaling of the probability of slip sizes, evidencing the complexity of the system under study. In a recent paper [5], we showed that the frictional behavior of squalane films under shear is also governed by long memory *distances* (as well as *times*), indicating the presence of large domains or long-range cooperativity (compared with molecular dimensions) in the film, as was suggested before by Demirel and Granick [22]. We also reported that squalane thin films under shear behave very similarly to other branched hydrocarbon liquids, such as poly-alpha olefine (PAO, a branched ''star-shaped'' molecule) and Exxsyn (a multiply branched polydisperse liquid), which are good models of lube oils [5].

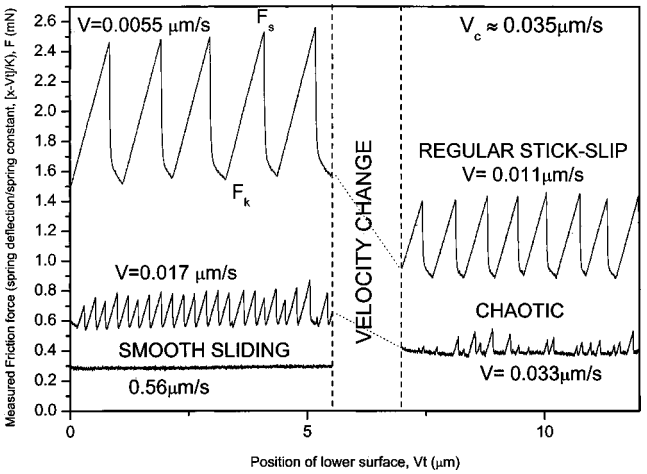

FIG. 2. Friction traces $F(t)$ obtained at different sliding velocities V for squalane films of thickness $D \sim 1.5$ nm. The continuous nature of the stick-slip to smooth sliding transition is evident. Other experimental conditions are $L = 1.5$ mN, $K = 1900$ N/m, and $T = 26$ °C.

Concerning static force measurements, the results by Granick *et al.* [22] and computer modeling by Landman *et al.* [37] of the branched liquid squalane, and our more recent work [5] with squalane, PAO, and Exxsyn, show them to have no short-range oscillatory force but a smooth monotonic repulsion. This is in marked contrast to more symmetrically shaped liquids such as cyclohexane, octamethylcyclotetracycloxane (OMCTS), and hexadecane, which exhibit short-range oscillatory force profiles, with multiple adhesive minima. One may ask whether these differences in the *static* forces are related to the differences in the *dynamic* (shear, lubrication) forces of these liquids under confinement. We may also ask whether these differences are fundamental, i.e., qualitative rather than simply quantitative. These are important questions because branched hydrocarbon fluids are the major component of base lube oils. We expect that studying the behavior of branched liquids such as squalane in detail will improve our understanding of the performance of real lubes under shear. We return to address the question posed above at the end of the paper.

RESULTS AND DISCUSSION

Special features of the stick-slip to smooth sliding transition

A reproduction of a measured friction trace for squalane at different driving velocities is shown in Fig. 2. As can be observed in the figure, with increasing velocity, there is a continuous transition from highly regular stick-slip to smooth sliding above some critical velocity V_c. Between these two regimes, there is a velocity range in which neither phase prevails: irregular stick-slip events of different spike

heights, duration, and frequency are observed, sometimes with long periods of relatively smooth sliding in between. This behavior, which has been observed before for different branched hydrocarbon systems [5,23], is very different from what is observed with simpler liquids such as spherical molecules or short-chained linear hydrocarbons that show a discontinuous ''first-order'' transition from stick slip to smooth sliding [23–25]. For simple liquids it has also been observed that the stick-slip spikes are always finite and have roughly the same magnitude regardless of how far the driving velocity V is from the critical velocity V_c of the transition. This does not seem to be the case with branched hydrocarbons that display a continuous reduction of the spike height as the phase transition is approached [5]. However, a similar continuous transition from stick-slip to smooth sliding via a chaotic regime was predicted for simple spherical molecules by computer simulations [11], suggesting perhaps that under different conditions (of load or temperature) even simple spherical molecules may exhibit this type of behavior.

In tribological experiments of simple liquids, it is customary to designate the velocity at which the stick-slip to smooth sliding transition occurs as the critical velocity, V_c [16]. Because of the continuous nature of the transition observed in this work, a different definition for V_c has to be found. Here we define V_c as the velocity above which no more stick-slip events are observed (above the noise).

Changing the driving velocity is not the only way of inducing the dynamic transitions. As mentioned before, load, temperature, and spring stiffness also determine the boundaries of the friction phase diagram. Figure 3 shows the dependence of V_c on these variables for thin films of squalane. In general, it was observed that V_c increases dramatically with increasing temperature and, much less dramatically, with decreasing load, suggesting the presence of a thermally activated process in the phase transition. Increasing the stiffness K of the friction force measuring spring also reduced the value of V_c, as can be observed in Fig. 3(b). Some variability in V_c was observed between experiments under the same conditions (within a factor of 3), indicating that other noncontrolled variables also affect the observed transition. Strong candidates are the elastic properties of the surfaces, small variations in temperature [cf. Fig. 3(a)], variations in the contact area, and the crystallographic orientation between the two surfaces. Experiments attempting to address these factors are currently in progress.

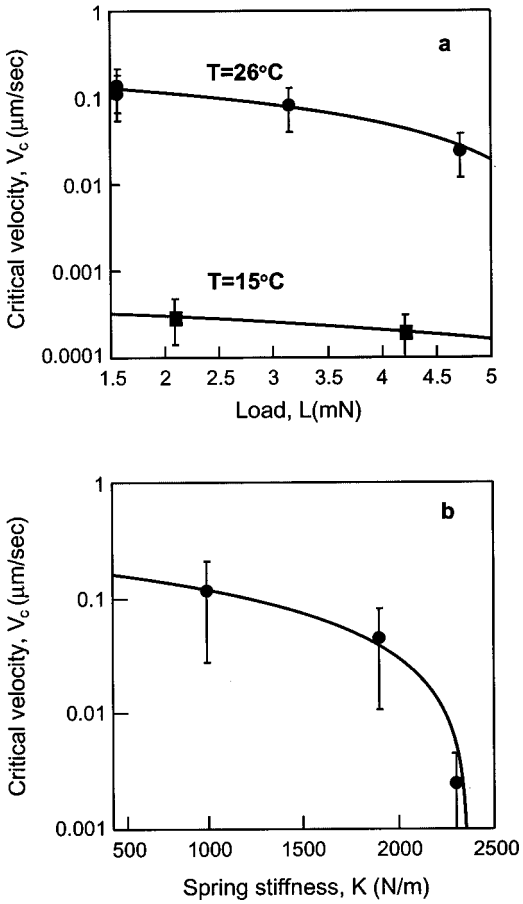

FIG. 3. Variation of the critical velocity, V_c, with experimental conditions. (a) Influence of normal load L and temperature T at fixed spring stiffness $K=1900$ N/m. (b) Influence of varying spring stiffness K at fixed $T=26\,^{\circ}$C and $L=1.5$ mN.

Characteristics of the stick-slip regime

The shapes of the stick-slip spikes also change with driving velocity, as can be observed in Fig. 4. At low sliding velocities ($V<V_c$), when regular stick slip is observed, two well-differentiated time scales can be observed in the slip part of the cycle. The slip can be fitted by a double exponential decay function, as presented in Fig. 4(a). A similar result was reported by Berman *et al.* [17] for thin films of hexadecane under overdamped conditions. Rozman *et al.* [14] obtained similar (theoretical) results for a simple model of a chain molecule with $N=15$ identical particles confined between two corrugated walls.

As the driving velocity approaches V_c, the stick-slip events cease to be regular, and cycles of many different sizes and lengths are observed. A typical stick-slip pattern is presented in Fig. 4(b). Slip in this regime can typically be described by a single exponential decay function (although occasionally two time scales are clearly observed) with the characteristic time of the decay, τ, varying from one cycle to the next. The measured τ is always much longer than τ_{mech} (which in this case is 7.6 ms), indicating that the dynamics is dominated by the slower relaxation times associated with the boundary layer. The long τ times measured seem to indicate that cooperative phenomena are responsible, because no conceivable single molecule relaxation time scale could account for the long decay times observed. It is also observed that the spring force does not always decay to the same value after successive slip events, in contrast to what is observed in the regular stick-slip regime.

During any particular stick-slip cycle (at any driving velocity), the relative velocity between the surfaces, V_i, goes from almost zero (stick) to a maximum value during the slip and back to zero again (stick). It is instructive to consider how the instantaneous (real) friction force between the surfaces, F_i, varies with their relative velocity, V_i. The results for different driving velocities, calculated by solving Eq. (1),

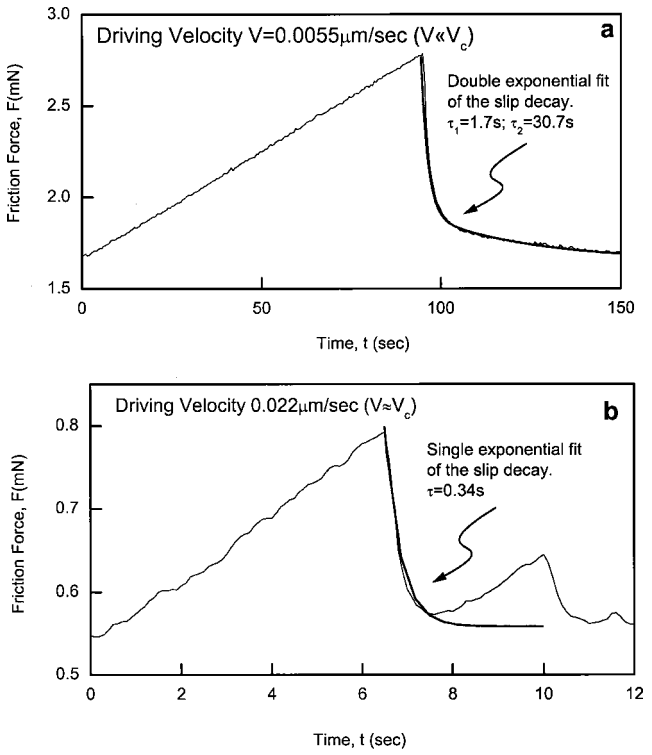

FIG. 4. Shapes of individual stick-slip spikes (a) far from V_c (b) close to V_c. Experimental conditions are $L=1.5\,\mathrm{mN}$, $K=1900\,\mathrm{N/m}$, and $T=26\,^{\circ}\mathrm{C}$.

are presented in Fig. 5. The instantaneous friction force is plotted as a function of time and the relative velocity between the mica surfaces, V_i. In general, it can be observed that the instantaneous friction force F_i is a multivalued function of V_i, being larger in the accelerating part of the slip than in the decelerating one. A similar result was reported by Nasuno *et al.* [26] in a study of dry friction of sand, and by Rozman *et al.* [14] based on a minimalistic model of a confined spring bead chain. We have reported before [5] that an instantaneous (transient) viscous response in the friction force is always observed with squalane and other branched lubricants when the driving velocity is changed: if the shear rate is suddenly increased (decreased), the friction force immediately increases (decreases). It is therefore not surprising to find that the measured instantaneous force is higher in the accelerating part of the stick-slip cycle.

The F-V phase profile changes dramatically with driving velocity near V_c. At low driving velocities [Fig. 5(a)], a limit cycle is clearly observed where different stick-slip events are represented by the same curve in the F-V space. As the driving velocity is increased closer to V_c, the shape of each loop changes from one cycle to the next [Fig. 5(b)], revealing the emergence of different time scales. With a further increase in V, over a certain velocity range, the measured frictional force displays chaotic behavior, and the phase portrait suggests the presence of a strange ''attractor'' [27] [Fig. 5(c)]. If the velocity is increased even more, the spring deflection fluctuates randomly [Fig. 5(d)], without any indication of any regular events in time.

To quantitatively determine the ''degree of stochasticity'' [27] of the system, we calculated the largest Lyapunov exponent, λ, of the spring deflection data. Essentially, this exponent is an average value of how quickly two trajectories with very close initial conditions diverge from each other. It measures how fast a perturbation grows or decays exponentially with time. A positive λ is usually associated with chaotic behavior [27].

The results obtained using the algorithm proposed by Wolf *et al.* [28] are presented in Fig. 6. They seem to confirm the presence of a chaotic region near the dynamic phase transition. This result has some direct implications for the functional form required for the frictional force, F_i. First, it must be a nonlinear function of time if chaotic behavior is to emerge from Eq. (1). Second, it is also known [27] that a three- or higher-dimensional space is necessary for chaotic behavior to be possible.

A chaotic response of surfaces during sliding was also observed in computer simulations by Thompson and Robbins [11] with confined spherical molecules, and by Rozman *et al.* [14] in their modeling of the behavior of a chain molecule of identical segments between two corrugated surfaces. Despite the relative simplicity of the system modeled in [14], some analogies between the two experiments can be established. Their spectrum of Lyapunov exponents is somehow more complicated than that reported in this paper, mainly because a greater extension of the space of parameters was explored in the simulations. Nevertheless, they also observed a chaotic stick-slip regime within a narrow window of sliding velocities near V_c.

Stop-start experiments

Variations in the friction following sudden changes in sliding conditions have been extensively studied in the past; these are known as ''stop-start'' or ''stiction'' experiments [5,16,24,29]. In stop-start experiments, the sliding is stopped for a certain amount of time, and then resumed at the same or different driving velocity. Following the evolution of the transient friction forces during an experiment provides useful information about relaxations within the sheared film. Of special interest is the *stiction* spike, $\Delta F=(F_s-F_k)$, measured on restarting. As has been reported before, very different results are observed for ΔF for simple and complex fluids [16,24]. Simple liquids, composed of spherical or short linear molecules, display an abrupt and finite stiction force [16] once the resting (or stopping) time is longer than a certain characteristic relaxation or latency time, τ_c. This characteristic time also depends on the load, temperature, and the previous driving velocity (*before* stopping), as was reported by Yoshizawa and Israelachvili [16]. It is almost an all or none response, with only a small increase in the stiction spike height observed for longer resting times ($t>\tau_c$).

In contrast, the stiction spikes ΔF of more complex fluids composed of branched or irregularly shaped molecules grow slowly and continuously with the stopping time [5,29]. As an example of what is observed, typical results for the stiction spikes as a function of stopping times for hexadecane and squalane are presented in Fig. 7. For squalane films, the stic-

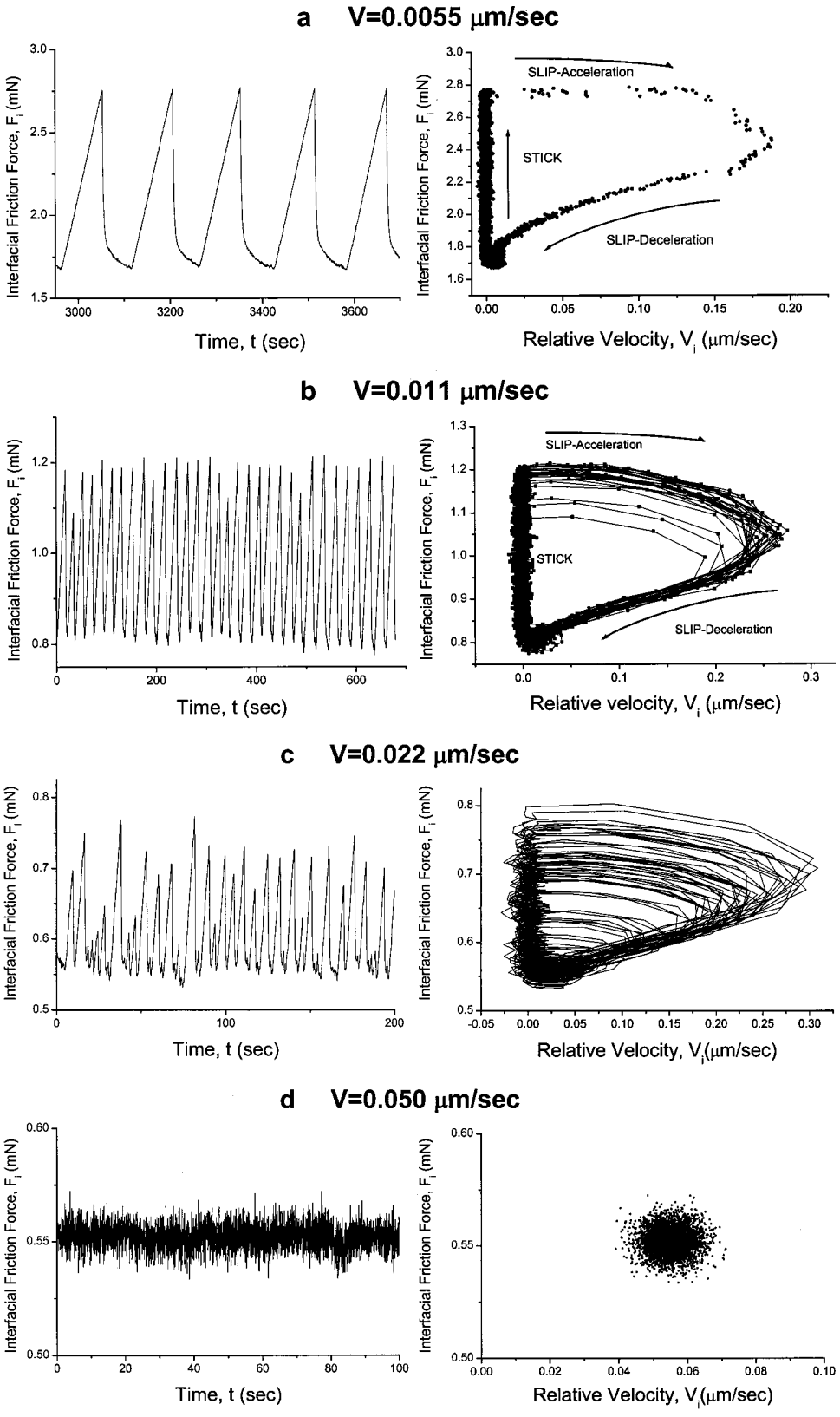

FIG. 5. Measured friction forces as a function of time t and relative surface velocity V_i. Experimental conditions are $L = 1.5$ mN, $K = 1900$ N/m, and $T = 26\,^{\circ}$C.

tion spike shows a continuous and logarithmic growth with waiting time, once the latency time, τ_c, is exceeded. As observed for simpler liquids, this latency time depends on the experimental conditions [5,16,29]. Similar results have been reported for different systems, such as fluorocarbon monolayers [29] and thin films of perfluoropolyether [30]. Given that we cannot measure a stiction spike smaller than our detection limit (around 10 μN), the determination of the latency time for these systems depends on the experimental setup. As discussed below, these results are intimately re-

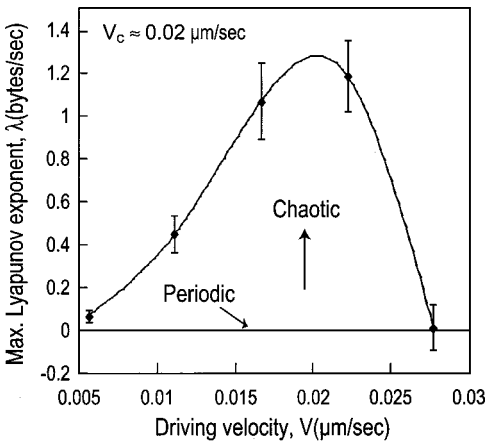

FIG. 6. Velocity dependence of the most positive Lyapunov exponent of the time evolution of the friction force. A positive Lyapunov exponent indicates that the orbit is unstable and that the trajectory diverges. Chaotic signals must have at least one positive exponent. For periodic orbits, all exponents are negative. Close to a bifurcation, the largest Lyapunov exponent tends toward zero. A maximum of the Lyapunov exponent is observed at the critical velocity, V_c.

lated to the smooth to stick-slip sliding transitions at different sliding velocities.

FURTHER ANALYSIS OF STICK-SLIP TO SMOOTH SLIDING TRANSITIONS

The observed characteristics of the stick-slip to smooth sliding transitions of short chain linear and branched lubricants appear to be correlated with, and can be explained in terms of, the stop-start stiction forces, which are themselves manifestations of the evolution of the dynamic phase state or structure of the molecules in the confined liquid films.

Relationship between stop-start behavior and stick-slip sliding of simple liquids

We first consider what happens in a stop-start experiment when smooth sliding ($V>V_c$) is stopped for a time t_s, then resumed at the same or a different velocity V. During the resting period, the externally applied stress may be reduced to zero ($F=0$) or allowed to remain at the kinetic value F_k. We introduce a system parameter—the *threshold* friction force, F_t—that differs from the *interfacial* friction force F_i in a subtle way: F_t is the ''potential'' friction force that would be required to initiate sliding (it does not imply that any sliding is actually taking place), while F_i is the actual instantaneous force experienced during sliding that appears in the equations of motion, Eqs. (1)–(3). When the drive is reactivated, no relative movement *between* the surfaces is initially observed: the surfaces remain stuck until the spring force F, which increases at a rate KV, equals the threshold friction force, F_t. Actually, some creep often occurs before sliding starts, but we will ignore creep effects at this level of approximation. The experimental conditions determine how the spring deflection, i.e., the measured force F, evolves with

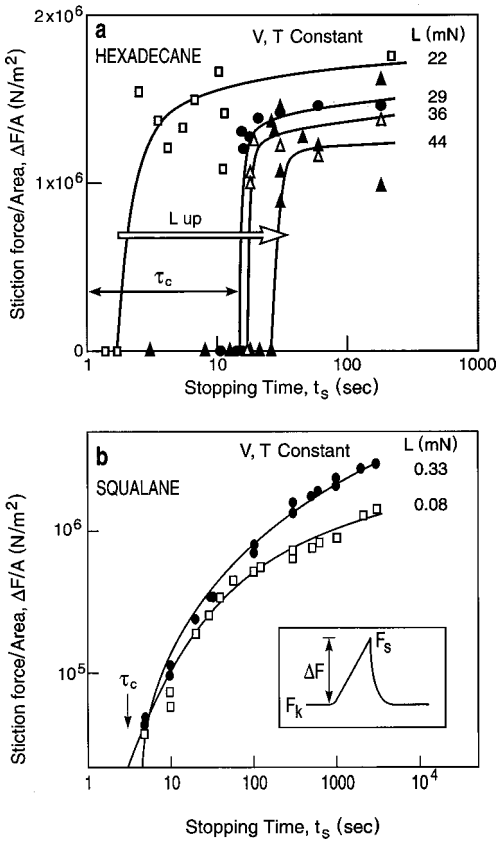

FIG. 7. Stiction height as a function of waiting time for different hydrocarbon lubricants at $T=26\,^{\circ}$C. (a) Hexadecane (from Ref. [16]). (b) Squalane (this work).

time after the commencement of sliding. This process is represented graphically in Fig. 8(a), where the threshold friction force F_t and the measured force F are plotted as a function of time t. Similar diagrams have been presented before by Rabinowicz [31], Persson [32], and Berman *et al.* [33]. For simple liquids, F_t may be represented as a simple step function, with $F_t=F_k$ at times shorter than the latency time τ_c after stopping [curve *b* in Fig. 8(a)] and $F_t=F_s$ at longer times [curve *c* in Fig. 8(a)].

If the stopping time t_s is short and/or the resumed driving velocity V is large, the spring force, which grows at a rate $dF/dt=KV$, will reach $F_k(=F_t)$ *before* the latency time, τ_c. If the spring stress during the resting period is zero, this will occur for

$$KV(\tau_c-t_s)>F_k \tag{4}$$

or

$$t_s<\tau_c-F_k/KV \tag{5}$$

and the measured friction force will rise monotonically to F_k and remain at this value as the surfaces slide, as illustrated in Fig. 8(b). For longer stopping times or lower driving velocities, i.e., for $t_s>\tau_c-F_k/KV$, the measured friction force will rise monotonically to F_s before the surfaces begin to slide. In this case, a stiction spike will be measured followed

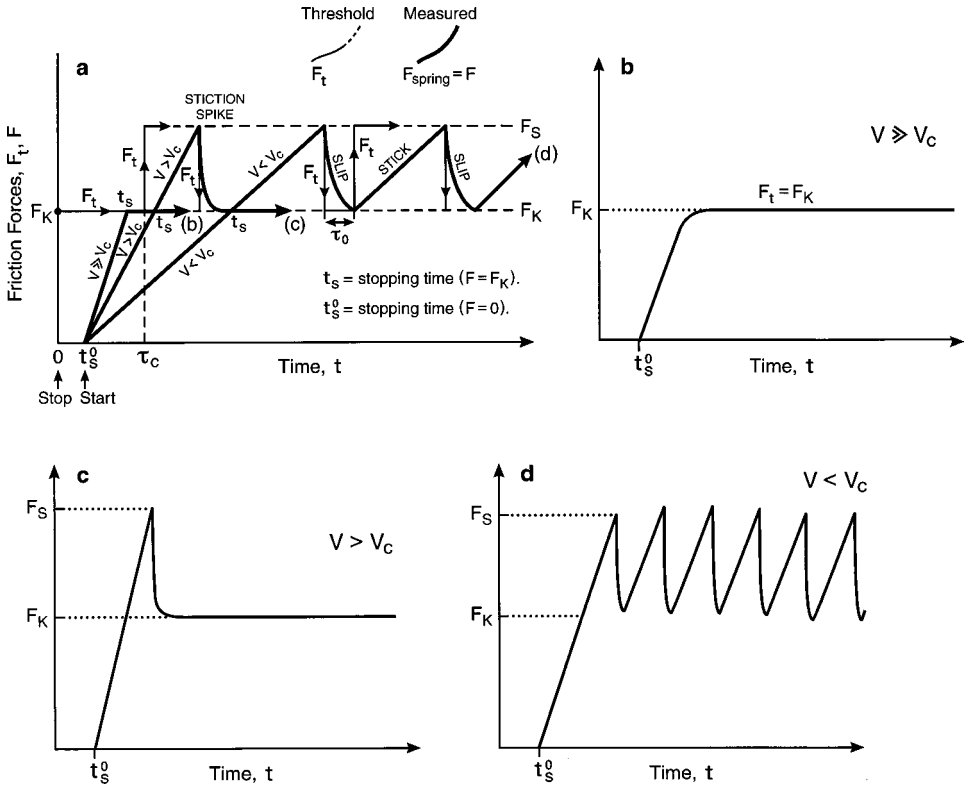

FIG. 8. Relation between stiction and the stick-slip to smooth sliding transition for simple liquids. Panel (a), measured force F and threshold friction force F_t as a function of time t for *overdamped* conditions after the film is kept at rest under zero stress for $V \gg V_c$ [curve *b* and panel (b)], for $V > V_c$ [curve *c* and panel (c)], and for $V < V_c$ [curve *d* and panel (d)]. Panels (a) and (b) here also correspond to panels (a) and (b) in Fig. 9 for squalane films for *underdamped* conditions.

by either smooth sliding at F_k [Fig. 8(c)] or stick-slip sliding [Fig. 8(d)], depending on whether $V > V_c$ or $V < V_c$.

If the spring stress during the resting period is not relaxed to zero but kept close to F_k, the above equations simplify to

$$t_s < \tau_c \quad \text{for smooth sliding on restarting} \tag{6}$$

and

$$t_s > \tau_c \quad \text{for a stiction spike on restarting.} \tag{7}$$

Figure 8(c) illustrates the expected evolution of the spring deflection on restarting at $V > V_c$ when condition (4) is not fulfilled: F first reaches F_s and then decays to F_k. For overdamped conditions, the monotonic decay from F_s to F_k will be determined by the relaxation time(s) of the confined film, τ_{film}. For underdamped conditions, the spring force will display transient oscillations of period τ_{mech} around the mean value before reaching the steady-state value of F_k.

Figure 8(d) illustrates the evolution of the spring deflection on restarting at $V < V_c$, where the initial stiction is followed by regular stick-slip sliding. During each stick-slip event, the film switches between the two different frictional states. There are several reasons to expect that the time τ_0 for a film to switch from the low friction, more ''fluid,'' state when it is being sheared (i.e., during stick-slip sliding) to the high friction state will be longer than the latency time τ_c for this transition under static conditions (i.e., during the resting period in a stop-start experiment). First, during sliding, energy is constantly being fed to the film at a rate proportional to $F_k V$ (the rate of frictional energy dissipation). Second, the lubricant layer is being continuously replenished during sliding, with fresh molecules entering into the contact at all times. Yoshizawa and Israelachvili [16] reported that the latency times τ_c for linear alkanes in stop-start experiments depend on the driving velocity V, with longer times observed for higher sliding velocities by a factor of ~5. In our experiments with the branched hydrocarbons squalane, PAO, and Exxsyn, we found very similar trends, and also that the latency time depends on the applied shear stress during the resting period [5]. We may expect that longer latency times τ_c in the stop-start experiments will probably imply longer latency times τ_0 under sliding conditions, but that in general $\tau_0 > \tau_c$.

Squalane and branched hydrocarbons

As described before, the transition from stick-slip to smooth sliding is significantly different for branched hydrocarbon films compared to films of simple spherical or short chain linear molecules. Nevertheless, the experimental observations can be explained, at least at a qualitative level, by constructing a diagram equivalent to the one presented in the preceding section. This is shown in Fig. 9(a), where the frictional force and the spring forces are plotted as a function of time in a typical stop-start experiment, and where the film is kept at zero stress during the resting phase. The static threshold friction force, $F_t(t)$, is expressed by the empirical function

$$F_t(t) = F_k + A \ln\left(1 + \frac{t}{\tau_0}\right), \tag{8}$$

where A is an adjustable constant and τ_0 is a characteristic time describing the evolution of the static threshold friction force under sliding conditions. This equation gives a good

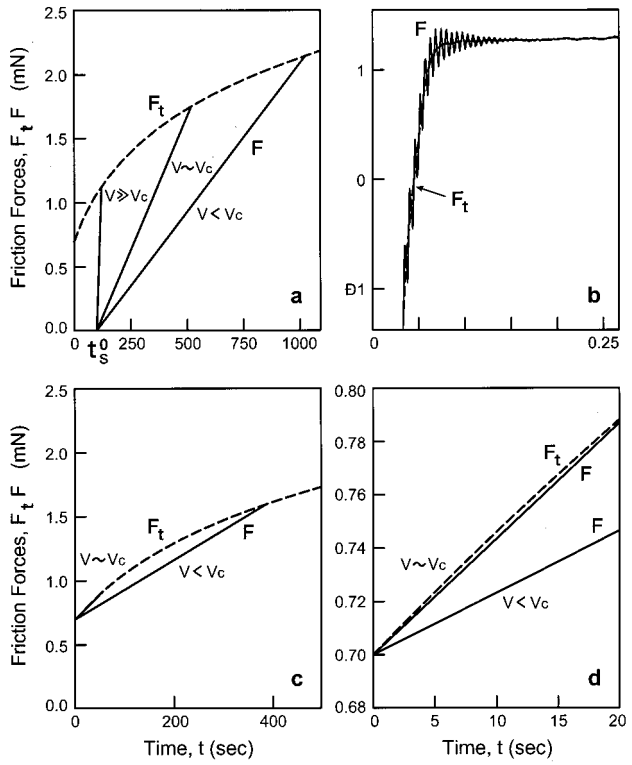

FIG. 9. Relation between stiction and the stick-slip to smooth sliding phase transition for squalane. (a) Measured force F (bold line) and threshold friction force F_t (dotted line) as a function of time after driving starts. The static threshold force, F_t, is calculated by fitting Eq. (13) to the measured stiction force vs time, as described in the text. The measured spring force is calculated as $F=KVt$, with $K=1300$ N/m and $V=0.001$, 0.0018, 0.022, and 0.20 μm/s. $V_c=0.0019$ μ/s under these conditions. A stiction spike was observed for all but the highest driving velocity. (b) Spring force (bold line) and friction force (dashed line) at *underdamped* conditions, for $V \gg V_c$. $V=55.5$ μm/s, $K=1900$ N/m, $L=1.5$ mN, and $T=26\,^{\circ}$C. (c) and (d) Measured force (bold line) and frictional response (dotted line) as a function of time after the initial stiction spike. The conditions are identical to (a). Only the two slowest velocities are shown. When driven at faster velocities, the deflection of the spring is constant, with $F=F_t=F_k$.

approximation of the observed temporal evolution of the frictional force with resting time t [cf. Fig. 7(b)]. It was first proposed by Dieterich [34] to describe the static friction forces in rocks, then refined by Ruina [10], and it has proven to accurately describe the behavior of the static forces in many systems, including rock surfaces [10,34], paper surfaces [35], polymer surfaces [36], and the fluid-lubricated surfaces studied here [5].

Arguments based on the slow increase in the contact area of elastoplastic junctions have been used to obtain the functional form of Eq. (8). However, these arguments cannot be applied to the lubricant fluid systems used in the SFA experiments, which are typically conducted at a constant area of contact and where plastic deformations of the surfaces are absent. Nevertheless, even in the absence of a physical model that describes the experimental results, Eq. (8) is suitably accurate for the discussion that follows. As an aside, different functional forms, for example a logarithmic function with a latency (or finite delay) time τ_c added, give a better fit to the measured data with the same number of parameters, especially at short resting times (cf. Fig. 7).

For analogous reasons given in the discussion of the preceding section, it is expected that τ_0 in Eq. (8) will be larger than τ_c, the characteristic time measured when the film is at rest. The value of τ_0 used in Fig. 9(a) was chosen to be 150 s in order to match the measured critical velocity, as described later. This dynamic relaxation time τ_0 is about nine times larger than the value of τ_c measured under static conditions at the same temperature and load, which may be compared with the value of $\tau_0/\tau_c \sim 5$ reported by Yoshizawa and Israelachvili for hexadecane [16].

At high driving velocities ($V > V_c$), the measured spring force will quickly match the frictional resistance, and the observed time evolution will be similar to what is observed with simple liquids: For overdamped conditions, the measured force will be a monotonic function of time, with a steady value equal to the kinetic friction force, F_k [Fig. 8(b)]. For underdamped conditions, the force will oscillate around the mean value before reaching the steady-state condition, F_k. Figure 9(b) presents the measured spring force, F, for a squalane film at a driving velocity of 55 μm/s and underdamped conditions after reversing the sliding direction. As can be seen in the figure, oscillations on the spring response having a frequency of $180\,\mathrm{Hz} = \tau_{\mathrm{mech}}^{-1}$ are present. If the inertial term in Eq. (2) is subtracted from the observed signal, the calculated frictional force displays a monotonic evolution to the steady state, as described above [dashed line in Fig. 9(b)].

At lower driving velocities, but still higher than V_c, a stiction spike can be initially observed before the spring force equals the kinetic friction force, and smooth sliding is recorded. The observed friction trace is identical to what is presented in Fig. 8(c). At driving velocities well below the critical velocity V_c, the observed spring response is again similar to that observed with simple liquids, and the spring force response will be as shown in Fig. 8(d). After the spring restoring force equals the threshold force F_t, the thin film changes to the low frictional state, and the elastic energy of the spring is converted to internal energy of the film and eventually dissipated, as discussed before. When F_t starts to grow again, the spring will not deflect fast enough to oppose the friction force, and the surfaces will be stuck again. After a few stick-slip cycles, the system will reach steady-state conditions.

The chaotic regime near the critical velocity

The distinctive behavior of branched hydrocarbon films appears when the driving velocity is close to V_c. The evolution of the stiction force with time is substantially slower for films of branched hydrocarbons than for simpler liquid films, as has been documented several times before [5,16,23] and presented in Fig. 7. The static threshold friction force, a well-defined value for simple liquids, evolves slowly in time in branched hydrocarbons. As can be observed in Figs. 9(c) and 9(d), there is a velocity range in which the evolution of

F_t and the load of the spring may have very similar slopes, lying almost parallel to each other. A small perturbation, fluctuation, or change in the sliding velocity or average time of confinement will then result in a large change on the static force necessary to initiate sliding of the surfaces. Thus, it is expected that the spring response will be extremely sensitive to noise and initial conditions when driven close to V_c. In practice, the sliding velocity and other system parameters can be controlled only within a certain range of accuracy and any small fluctuation will suffice to significantly change the time necessary for the spring force and the threshold friction forces to match, and that difference in time will translate into a significant fluctuation in the size of the stick-slip event [cf. Fig. 9(c)].

The range of velocities in which this near-tangent crossing behavior is observed corresponds with the observed V_c for the experimental conditions of Fig. 9, which is 0.0019 μm/s. However, it is important to mention that the values of the frictional resistance are extremely sensitive to the arbitrarily chosen τ_0. This near-tangency between the spring and the threshold friction curves [cf. Fig. 9(c)] is the reason for the great variability and chaotic (rather than random or stochastic [27]) behavior of the observed response signal.

Physical interpretation/description

It is clear that the important question to ask is what is the origin of the difference in the time scales and time evolution of F_t of thin films of linear and branched hydrocarbons under confinement. This difference is the reason for the distinctive behavior observed, and is ultimately responsible for the superior lubricity properties of branched hydrocarbons. One possible explanation can be gleaned from molecular-dynamics simulations of confined films of hydrocarbons of different complexity. Gao and co-workers [37] found that squalane does not layer when confined between two flat surfaces in the same way as linear hydrocarbons. They found that interlayer interdigitation in squalane and other branched hydrocarbon films is substantially larger than with linear hydrocarbons. Because of this, long-range cooperative effects are more likely to be present and longer correlation times and lengths can be expected.

State of the art molecular-dynamics simulations cannot yet give all the answers to this problem. The extremely long time and length scales present [5] make the complete problem almost unmanageable using MD simulations. To achieve a complete description of the phenomena, a different or complementary approach will have to be taken. An interesting model proposed by Persson [12], in the spirit of the Burridge-Knopoff [13] spring-block model, attempts to capture some of the physics that emerges from the experimental results. Persson [12] included the influence of thermal processes, and suggested that two-dimensional fluid and/or frozen domains nucleate and grow or disappear in the lubricant film during sliding and stopping. By simulating these islands as coupled oscillators, many features observed in the experiments can be reproduced. Of particular interest is the possibility of aggregates of different sizes being present in the contact region, and the natural emergence of a broadband spectrum of relaxation times, which is very consistent with our experimental results.

However, the simulation of Thompson and Robbins [11] of confined simple, spherical molecules also showed a continuous transition from stick-slip to smooth sliding via a chaotic regime, which suggests that under different conditions (of load or temperature) even simple spherical molecules may exhibit the type of behavior observed so far only with more complex fluids. And Rozman *et al.* [14] proposed the use of an extremely simple model that also seems to reproduce some of the results presented here: complexity and chaotic behavior is predicted with a model consisting of nothing more than a spring-bead molecule confined within a corrugated potential. Nevertheless, as mentioned before, the connection between the model parameters and the experimental variables is not clear at this point.

A different approach was proposed by Carlson and Batista [9], by introducing the idea of using ''rate and state'' models [10] to describe the temporal evolution of sliding boundary lubricated surfaces. However, the one-dimensional state variable currently used in the ''rate and state'' model cannot account for all the observed effects; at least one additional state variable will be needed to produce an adequate description of the results. A common drawback of these phenomenological models is the lack of a physical meaning for the variables used in the equations. To achieve a satisfactory description of the phenomena, it will be desirable to map those variables into the real molecular or material properties of the systems.

SUMMARY AND CONCLUSIONS

The nature of the observed dynamic phase transition between stick-slip and smooth frictional sliding for branched hydrocarbon molecules was studied in detail in this and a previous paper [5]. The results were compared with the similar transition observed in simple and short chain linear hydrocarbon liquids. The relation between the temporal evolution of the threshold friction force and the measured stick-slip to smooth sliding transition was established for both simple and branched hydrocarbon lubricants. The slow evolution of thin films of branched hydrocarbons to their steady-state sliding state, when compared with simpler hydrocarbons, was found to be responsible for the distinctive features of the observed dynamic phase transitions, which, for branched liquids, include a chaotic stick-slip regime over a narrow window of velocities. This slow approach to steady state appears to be associated with the presence of large, metastable multimolecular domains in the system having a broadband of relaxation times.

Concerning other differences between liquids of different molecular architecture, multiply branched hydrocarbon liquids such as squalane, poly-alpha olefine (PAO), and Exxsyn have been found to exhibit no short-range oscillatory force (with multiple adhesive minima) but a smooth monotonic repulsion [5,22,37]. This is in marked contrast to more symmetrically shaped liquids such as cyclohexane, OMCTS, and hexadecane, which exhibit short-range oscillatory force profiles. Our results further show that molecularly thin films

of these three branched liquids make very gradual or ''continuous'' transitions to steady-state sliding (taking $>10^4$ s), whereas cyclohexane and hexadecane make abrupt transitions that resemble ''discontinuous'' first-order-like transitions. One may ask whether the differences in the *static* forces are related to the differences in the *dynamic* (shear, lubrication) forces of these liquids under confinement, and also whether these differences are qualitative rather than quantitative. For example, is it possible that multiply branched and other highly irregularly shaped liquids simply have longer relaxation times and larger characteristic length scales, or that the properties can be made to coincide under different conditions of load, sliding velocity, or temperature? These questions have important practical implications because experience has shown that highly branched molecules produce the best low-friction lubricant fluids. Our limited results do not allow us to say whether the differences are ''fundamental,'' but certainly under the limited range of conditions (of load, temperature, sliding velocity, and contact area) studied so far, one would expect large differences in their performance as lubricant fluids.

ACKNOWLEDGMENTS

The authors thank Dr. D. Lavalle for many useful discussions. This work was funded by grants from INTEVEP S.A., Venezuela, Exxon Research and Engineering Company, Clinton, NJ, the Department of Energy under Grant No. DE-FG03-87ER45331 for the experimental work, and the Keck Foundation for the theoretical analysis.

[1] J. N. Israelachvili, Surf. Sci. Rep. **14**, 109 (1992), and references therein.
[2] C. M. Mate, G. M. McClelland, R. Erlandsson, and S. Chiang, Phys. Rev. Lett. **59**, 1942 (1987); R. Erlandsson, G. Hadziioannou, C. M. Mate, G. M. McClelland, and S. Chiang, J. Chem. Phys. **89**, 5190 (1988).
[3] J. Krim and A. Widom, Phys. Rev. B **38**, 12 184 (1988).
[4] J. A. Harrison and D. W. Brenner, in *Handbook of Micro/Nano Tribology*, edited by B. Bhushan (CRC, Boca Raton, FL, 1995), and references therein.
[5] C. Drummond and J. Israelachvili, Macromolecules **33**, 4910 (2000).
[6] D. Dowson, *History of Tribology* (Langman, London, 1979).
[7] A. Dhinogwala, L. Cai, and S. Granick, Langmuir **12**, 4537 (1996).
[8] M. L. Williams, R. F. Landel, and J. D. Ferry, J. Am. Chem. Soc. **77**, 3701 (1955); K. C. Ludema and D. Tabor, Wear **9**, 329 (1966); G. Luengo, J. Israelachvili, and S. Granick, *ibid.* **200**, 328 (1996).
[9] J. M. Carlson and A. A. Batista, Phys. Rev. E **53**, 4153 (1996).
[10] J. H. Dieterich, J. Geophys. Res. B **84**, 2161 (1979); A. Ruina, *ibid.* **88**, 10 359 (1983).
[11] P. A. Thompson and M. O. Robbins, Science **250**, 792 (1990).
[12] B. N. J. Persson, Phys. Rev. B **50**, 4771 (1994).
[13] R. Burridge and L. Knopoff, Bull. Seismol. Soc. Am. **57**, 341 (1967).
[14] M. G. Rozman, M. Urbakh, J. Klafter, and F.-J. Elmer, J. Phys. Chem. B **102**, 7924 (1998); see also M. Porto, M. Urbakh, and J. Klafter, Europhys. Lett. **50**, 326 (2000).
[15] F. P. Bowden and D. Tabor, *The Friction and Lubrication of Solids* (Clarendon, Oxford, 1964); F. P. Bowden and L. Leven, Proc. R. Soc. London, Ser. A **169**, 371 (1939).
[16] H. Yoshizawa and J. Israelachvili, J. Phys. Chem. **97**, 11 300 (1993).
[17] A. D. Berman, W. A. Ducker, and J. N. Israelachvili, Langmuir **12**, 4559 (1996).
[18] B. N. J. Persson, *Sliding Friction* (Springer-Verlag, Berlin, 1998).
[19] A. M. Homola, J. N. Israelachvili, M. L. Gee, and P. M. McGuiggan, J. Tribol. **111**, 675 (1989).
[20] G. Luengo, F.-J. Schmitt, R. Hill, and J. Israelachvili, Macromolecules **30**, 2482 (1997).
[21] J. Israelachvili, J. Colloid Interface Sci. **44**, 259 (1973); M. Heuberger, G. Luengo, and J. Israelachvili, Langmuir **13**, 3839 (1997).
[22] A. Demirel and S. Granick, Phys. Rev. Lett. **77**, 4330 (1996).
[23] J. Israelachvili, P. McGuiggan, M. Gee, A. Homola, M. Robbins, and P. Thompson, J. Phys.: Condens. Matter **2**, SA89 (1990).
[24] H. Yoshizawa, Y.-L. Chen, and J. Israelachvili, Wear **168**, 161 (1993).
[25] J. Carlson and A. Berman (private communication).
[26] S. Nasumo, A. Kudrolli, and J. P. Gollub, Phys. Rev. Lett. **79**, 949 (1997); S. Nasumo, A. Kudrolli, A. Bak, and J. P. Gollub, Phys. Rev. E **58**, 2161 (1996).
[27] A. H. Nayfeh and B. Balachandran, *Applied Nonlinear Dynamics* (Wiley Interscience, New York, 1994).
[28] A. Wolf, J. B. Swift, H. L. Swinney, and T. Pignataro, Physica D **16**, 285 (1985).
[29] S. Yamada and J. Israelachvili, J. Phys. Chem. **102**, 234 (1998).
[30] S. Hirz, A. Subbotin, C. Frank, and G. Hadziioannou, Macromolecules **29**, 3970 (1996).
[31] E. Rabinowicz, *Friction and Wear of Materials*, 2nd ed. (Wiley, New York, 1995).
[32] B. N. J. Persson, Phys. Rev. B **51**, 13 568 (1995).
[33] A. D. Berman, W. A. Ducker, and J. Israelachvili, in *Physics of Sliding Friction*, edited by B. N. J. Persson and E. Tosatti, *NATO Advanced Science Institute Series E* (Kluwer, Dordrecht, 1996), Vol. 311, pp. 51–67.
[34] J. H. Dieterich, J. Geophys. Res. **77**, 3690 (1972).
[35] T. Baumberger, F. Heslot, and B. Perring, Nature (London) **367**, 544 (1994); F. Heslot, T. Baumberger, B. Perrin, B. Caroli, and C. Caroli, Phys. Rev. E **49**, 4973 (1994).
[36] P. Berthoud, T. Baumberger, C. G'Sell, and J.-M. Hiver, Phys. Rev. B **59**, 14 313 (1999).
[37] J. Gao, W. D. Luedtke, and U. Landman, J. Chem. Phys. **106**, 4309 (1997); J. Gao, W. D. Luedtke, and U. Landman, Phys. Rev. Lett. **79**, 705 (1997).